



## Detection of Very High Energy Gamma-Rays from the BL Lac Object 1ES 2344+514 in a Low Emission State with the MAGIC Telescope

ROBERT WAGNER<sup>1</sup> AND MARKUS MEYER<sup>2</sup> FOR THE MAGIC COLLABORATION

<sup>1</sup> *Max-Planck-Institut für Physik, D-80805 München, Germany*

<sup>2</sup> *Universität Würzburg, Am Hubland, D-97074 Würzburg, Germany*

*robert.wagner@mppmu.mpg.de*

**Abstract:** The MAGIC telescope has observed very-high energy gamma-ray emission from the AGN 1ES 2344+514. A gamma-ray signal corresponding to an 11 sigma excess and an integral flux of  $(2.38 \pm 0.30_{\text{stat}} \pm 0.70_{\text{syst}}) \times 10^{-11} \text{ cm}^{-2} \text{ s}^{-1}$  above 200 GeV has been obtained from 23.1 observing hours between August 2005 and January 2006. The observations show a relatively steep differential photon spectrum ( $\alpha = -2.95 \pm 0.12_{\text{stat}} \pm 0.20_{\text{syst}}$ ) between 140 GeV and 5.4 TeV. No significant time variability has been observed.

### Introduction

In the past, most of the very-high energy (VHE)  $\gamma$ -ray emitting active galactic nuclei (AGN) were discovered during phases of high activity. It still remains an open question whether these are only temporarily active and are completely inactive between times of flaring, or if there exists a state of low but continuous  $\gamma$ -ray emission. The temporal and spectral properties of such a low emission state are still mostly elusive.

During the winter of 1995/6, the Whipple collaboration observed a  $5.8\sigma$  excess signal from the BL Lac-type AGN 1ES 2344+514. The measured flux was highly variable, with the most significant signal occurring during a single flare, while the remaining data combined led to an only marginal excess [1]. A deep 72.5h HEGRA exposure from 1997 to 2002 indicated a signal at a significance level of  $4.4\sigma$  [2].

Here we present MAGIC observations of 1ES 2344+514. We infer an  $E > 200$  GeV light curve and derive a  $\gamma$ -ray spectrum. We compare our measurements with with the all-time (1995-2005) VHE light curve. Further, SSC modeling is performed employing wide-range spectral energy distribution (SED) data.

### Observations

The observations were performed between August 2005 and January 2006 with the MAGIC telescope [3]. Its essential parameters are a 17 m diameter mirror of parabolic shape and a  $\approx 3.5^\circ$  diameter field of view PMT camera. 1ES 2344+514 was observed for 32 hours in total under zenith angles from  $23^\circ$  to  $38^\circ$ . The observations were carried out in wobble mode, i.e. by alternately tracking two positions at  $0.4^\circ$  offset from the camera center. The KVA optical telescope conducted simultaneous  $R$ -band observations.

### Data Analysis

The data analysis was carried out using the standard MAGIC analysis software [4] and is described in detail elsewhere [5]. After data quality cuts, 23.1 h worth of data remained, for which image parameters were calculated [6]. These were subjected to a  $\gamma$ /hadron separation based on the Random Forest (RF) method [7]. The arrival directions of the showers in equatorial coordinates were calculated using the DISP method [8]. The energy of the primary  $\gamma$ -rays was reconstructed from the image parameters again using a RF method and taking into account the full instrumental energy resolution.

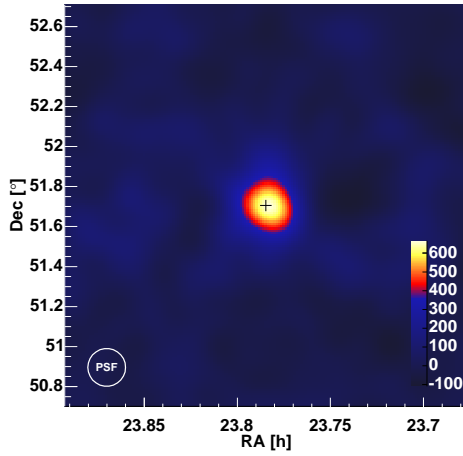


Figure 1: Smoothed excess event map for  $E_\gamma > 180$  GeV. The number of excess events is given in units of  $10^{-5}\text{sr}^{-1}$ . Black cross: expected source position.

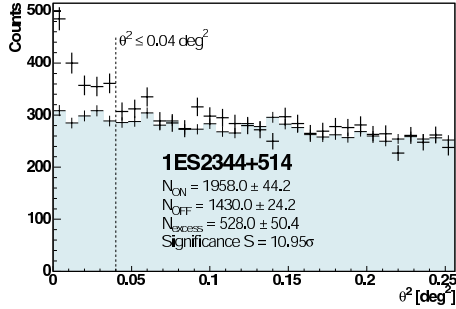


Figure 2:  $\theta^2$  plot for  $E_\gamma > 180$  GeV. Heavy crosses: On-events, small crosses: Off-source background.

Fig. 1 shows a sky map around the 1ES 2344+514 position. A clear point-like  $\gamma$ -ray excess is visible in the data, the maximum of which is within errors coincident with the location of 1ES 2344+514. To calculate the significance of the observed excess, the squared angular distance  $\theta^2$  between the reconstructed shower direction and the object position as shown in Fig. 2 is used. The observed excess signal of 528 events below  $\theta^2 < 0.04\text{deg}^2$  corresponds to a significance of  $11\sigma$  according to eq. 17 in [9].

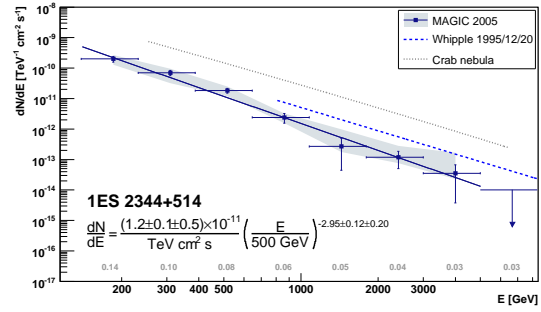


Figure 4: Differential photon spectrum for 1ES 2344+514. The gray band represents systematic errors coming from varying the  $\gamma$  efficiency in the determination of the spectrum.

The  $\geq 200$  GeV light curve (Fig. 3) shows small changes and trends beyond those expected from statistical fluctuations. The structure observed during MJD 53580–53600 is compatible with a constant-flux ansatz ( $\chi^2/\text{dof} = 6.1/6$ ), while from MJD 53726.82–53726.90 a flux of  $2.4\sigma$  above the average flux inferred from the surrounding days MJD 53720–53740,  $(1.8 \pm 0.6) \cdot 10^{-11}\text{cm}^{-2}\text{s}^{-1}$  ( $\chi^2/\text{dof} = 4.9/7$ ), was found. The average flux  $F(E > 200\text{GeV}) = (2.38 \pm 0.30_{\text{stat}} \pm 0.70_{\text{syst}}) \times 10^{-11}\text{cm}^{-2}\text{s}^{-1}$  corresponds to  $(10 \pm 1)\%$  of the Crab nebula flux in the same energy range. While previous VHE observations of 1ES 2344+514 did not allow short-term studies of temporal characteristics, with MAGIC, this level can now be detected with only a few hours of observations, enabling studies of the VHE  $\gamma$ -ray variability properties of this object over a significant part of its dynamical range. Thus, 1ES 2344+514 adds to the small group of blazars for which such studies are now possible on a diurnal basis—Mkn 421, Mkn 501 and PKS 2155-304.

The reconstructed spectrum after unfolding [10] (Fig. 4) can be fitted with a simple power law between 140 GeV and 5.4 TeV ( $\chi^2_\nu/\text{dof} = 8.56/5$ ) as

$$\frac{dN}{dE} = \frac{(1.2 \pm 0.1_{\text{stat}} \pm 0.5_{\text{syst}}) \cdot 10^{-11}}{\text{TeV cm}^2 \text{ s}} \times \frac{E}{500 \text{ GeV}}^{-2.95 \pm 0.12_{\text{stat}} \pm 0.2_{\text{syst}}}$$

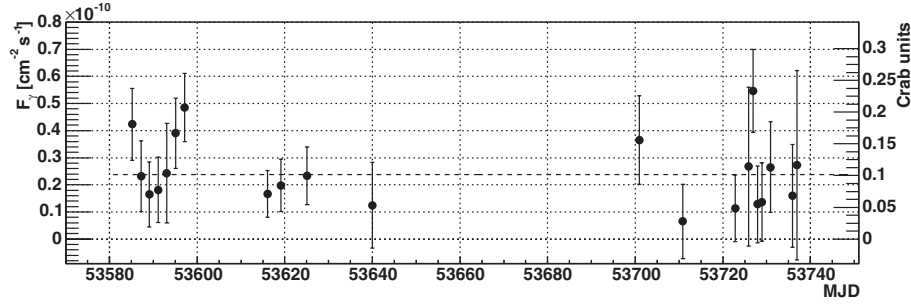


Figure 3:  $E > 200$  GeV light curve. Dashed line: average flux level of  $(2.38 \pm 0.30) \times 10^{-11} \text{cm}^{-2} \text{s}^{-1}$  ( $\chi_{\text{red}}^2 = 21.2/20$ ).

### Long-term VHE Light Curve

The VHE light curve in Fig. 5 was obtained by normalizing all known data to an integral flux  $F(E > 350 \text{ GeV})$ . The fluxes given in the literature were extrapolated, where necessary, using the spectral index found in this paper. All reported observations with significances below  $2.0\sigma$  ( $\approx 95\%$  probability) were converted to 99% upper flux limits.

In 1995/6, Whipple discovered 1ES 2344+514 at a flux level of  $(0.11 \pm 0.05)$  Crab units at  $E > 350 \text{ GeV}$ , except for the December 1995 flare, when  $(0.63 \pm 0.15)$  Crab units were obtained [16]. Follow-up observations by Whipple and HEGRA in 1996-8 yielded upper limits of 0.08 Crab units and 0.12 Crab units, respectively. In 1998 and 2002, the object was observed for almost 60 h by HEGRA resulting, when combined, in a flux of  $(0.042 \pm 0.012)$  Crab units at  $E > 930 \text{ GeV}$  [18], which translates to  $(0.053 \pm 0.015)$  Crab units when extrapolating to  $E \geq 350 \text{ GeV}$ . From observations of 1ES 2344+514 in 2002, the Whipple group could infer a low flux level of  $< 0.03$  Crab units with a marginal significance of  $3.1\sigma$  [17] at  $E > 400 \text{ GeV}$ .

While the Whipple and HEGRA measurements allowed to conclude on an emission level of  $\leq 11\%$  Crab units only after long observation times, the MAGIC observations are the first time-resolved measurements at this emission level for 1ES 2344+514. We find the flux of 1ES 2344+514 to be  $(0.054 \pm 0.006)$  Crab units for  $E > 350 \text{ GeV}$ , which is well in line with the HEGRA 1997-2002 evidence.

### Intrinsic Energy Spectrum

Having to traverse a cosmological distance ( $z = 0.044$ ), the  $\gamma$ -rays emitted by 1ES 2344+514 interact with EBL photons [11]. We use the “best-fit” EBL model of [12] to calculate the optical depth  $\tau_{\gamma\gamma}$ . With it, the intrinsic source spectrum is determined. It can be described by a simple power law of the form

$$\frac{dN}{dE_{\text{intr}}} = \frac{(2.1 \pm 1.2_{\text{stat}} \pm 0.5_{\text{syst}}) \cdot 10^{-11}}{\text{TeV cm}^2 \text{ s}} \times \frac{E^{-2.66 \pm 0.50_{\text{stat}} \pm 0.20_{\text{syst}}}}{500 \text{ GeV}}$$

between 140 GeV and 5.4 TeV ( $\chi_{\nu}^2 = 0.68/5$ ). The spectrum shows a tendency to flatten towards low energies. A fit with a logarithmic curvature term [13] shows a clear curvature and enables locating a spectral peak at  $E_{\text{peak}} = (202 \pm 174) \text{ GeV}$ .

### Spectral Energy Distribution

The SED for 1ES 2344+514 is shown in Fig. 6 along with a homogeneous one-zone SSC model fit [14] to the Whipple flare and the MAGIC data (intrinsic spectra are indicated by the dashed curves). BS96 and BS98 represent two *BeppoSAX* data sets taken during a quiescent state and simultaneously with Whipple observations, respectively. Optical KVA data and the RXTE-ASM upper limit were taken simultaneously with the MAGIC data. The dotted curve was fitted to the BS96/Wh96 observation. For references and model parameters see

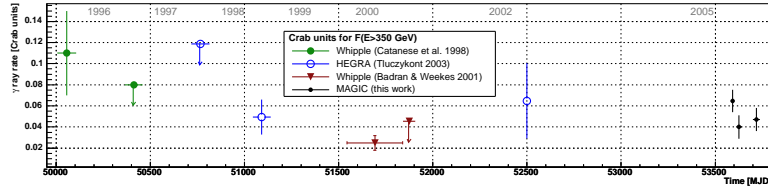


Figure 5: Overall VHE light curve for 1ES 2344+514 [16, 17, 2]. The 1995 December 20 flare has been excluded for clarity.

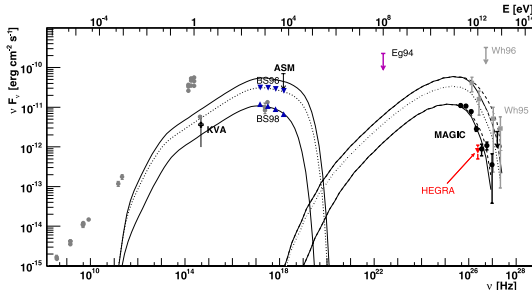


Figure 6: Overall SED during the Whipple 1995 flare (Wh95) and MAGIC observations. Wh96—Whipple upper limit. Eg94—EGRET upper limit. Gray data points—archival radio and optical data.

[5]. The size of the emission region  $R$  was chosen as to account for day-scale variability ( $R \leq \delta_{-1} \times t_{\text{days}} \times 2.48 \times 10^{16} \text{cm}$  with  $\delta_{-1} = \text{Doppler factor}/10$ ). While most of the obtained model parameters are compatible with the parameter space spanned by other models [15], the magnetic field strength found here is rather low (also found for Mkn 421 e.g. by [19]). We note that the presented SED models are rather speculative, given the non-simultaneity of the currently available data. Future multiwavelength campaigns on 1ES 2344+514 will hopefully improve this situation.

## Acknowledgments

We thank the IAC for the excellent working conditions at the Observatorio del Roque de los Muchachos in La Palma. The support of the German BMBF and MPG, the Italian INFN and Spanish CICYT is gratefully acknowledged. This work was also supported by ETH Research Grant TH 34/04 3 and by the Polish MNiI Grant 1P03D01028.

## References

- [1] Schroedter, M., et al., 2005, *ApJ*, 634, 947 and references therein
- [2] Aharonian, F. A., et al., 2004a, *A&A*, 421, 529
- [3] Baixeras, C., et al., 2004, *Nucl. Instrum. Meth.*, A518, 188; Cortina, J. et al. 2005, In *29th ICRC, Pune*, 5, 359
- [4] Bretz, T. & Wagner, R. M., 2003, In *28th ICRC, Tsukuba, Japan*, 5, 2947
- [5] Albert, J., et al., 2007, *ApJ*, 662, 892
- [6] Hillas, A. M., 1985, In *19th ICRC, La Jolla*, 3, 445
- [7] Breiman, L. 2001, *Machine Learning*, 45, 5; Bock, R. K., et al., 2004, *Nucl. Instrum. Meth.*, A516, 511
- [8] Domingo-Santamaría, E., et al., 2005, In *29th ICRC, Pune, India*, 4, 51
- [9] Li, T.-P. & Ma, Y.-Q., 1983, *ApJ*, 272, 317
- [10] Anykeyev, V. B., Spiridonov, A. A. & Zhi-gunov, V.B., 1991, *Nucl. Instrum. Meth.*, A303, 350; Mizobuchi, S., et al., 2005, In *29th ICRC, Pune, India*, 5, 323
- [11] Hauser, M. G. & Dwek, E., 2001, *ARA&A*, 39, 249
- [12] Kneiske, T. M., et al., 2004, *A&A*, 413, 807
- [13] Massaro, E., et al., 2004, *A&A*, 413, 489
- [14] Krawczynski, H., et al., 2004, *ApJ*, 601, 151
- [15] Kino, M., Takahara, F. & Kusunose, M., 2002, *ApJ*, 564, 97; Giommi, P., et al., 2002, arXiv:astro-ph/0209596
- [16] Catanese, M., et al., 1998, *ApJ*, 501, 616
- [17] Badran, H. M. & Weekes, T. C., 2001, In *27th ICRC, Hamburg, Germany*, 2653
- [18] Tluczykont, M. 2003, Ph.D. Thesis, University of Hamburg
- [19] Maraschi, L., et al., 1999, *ApJL*, 526, 81